CONFIDENTIAL

Copy
RM L53I09

NACA RM L53I09

NACA

RESEARCH MEMORANDUM

WAKE SURVEYS IN THE SLIPSTREAM OF A FULL-SCALE SUPERSONIC-TYPE THREE-BLADE PROPELLER AT MACH NUMBERS TO 0.96

By John M. Swihart and Harry T. Norton, Jr.

Langley Aeronautical Laboratory
Langley Field, Va.

NATIONAL ADVISORY COMMITTEE
FOR AERONAUTICS

WASHINGTON

October 30, 1953

CONFIDENTIAL

NATIONAL ADVISORY COMMITTEE FOR AERONAUTICS

RESEARCH MEMORANDUM

WAKE SURVEYS IN THE SLIPSTREAM OF A FULL-SCALE SUPERSONIC-TYPE THREE-BLADE PROPELLER AT MACH NUMBERS TO 0.96

By John M. Swihart and Harry T. Norton, Jr.

SUMMARY

An investigation of the thrust loading by wake surveys in the slipstream of a full-scale supersonic-type three-blade propeller has been conducted in the Langley 16-foot transonic tunnel. The propeller investigated was the Curtiss-Wright (design no. 109622) solid-steel three-blade propeller with symmetrical NACA 16-series airfoil sections which had a thickness distribution from 6 percent at the spinner to 2 percent at the propeller tip. The blade-angle range measured at the 0.75 radial station was from 45.4° to 60.2° over a Mach number range from 0.60 to 0.96.

The results of the investigation indicate that the integrated thrust-coefficient values are in good agreement with the force data. Operation at Mach numbers up to 0.89 at a blade angle of 50.8° measured at the 0.75 radial station and an advance ratio of 2.75 produced no severe compressibility losses in thrust loading, and the thrust coefficient decreased very slightly above a forward Mach number of 0.85. The losses in section thrust coefficient were more severe for the higher blade angles and advance ratios. The trend of the data indicates that the advance ratio and blade angle would have to decrease toward the design condition (advance ratio of 2.2 and about 45° blade angle) in order to obtain optimum efficiency.

INTRODUCTION

Propellers now in general use are constructed with moderately thick blade sections and are known to experience thrust and efficiency losses at high forward speeds. The investigations of references 1 and 2 have

indicated that higher efficiencies can be attained up to a Mach number of 0.925 by reducing blade-section thickness ratios to 5 and 3 percent. The propeller used in this investigation was designed to reduce the thrust and efficiency losses experienced by propellers with thicker blade sections and to provide efficient operation at supersonic blade-section speeds.

Wake surveys of the propeller slipstream have been used to give a clear picture of the blade-element loading in conjunction with force measurements and to provide thrust data in the absence of a force-measuring system. Extensive surveys have been made in reference 3 to determine the section lift-coefficient distribution of five full-scale propellers which have moderate to thick blade sections. Reference 4 presents the thrust loadings of model propellers obtained by wake surveys at Mach numbers up to 0.925.

The purpose of this paper is to present the thrust loadings from wake-survey measurements of a full-scale supersonic propeller at Mach numbers up to 0.96. These wake surveys of the propeller slipstream were made concurrently with the force measurements of reference 5. Thrust loadings are presented for the blade angle and Mach number range of the investigation and a comparison of the integrated thrust coefficients with force data is presented. The investigation covered a blade-angle range (measured at the 0.75 radial station) from 45.4° to 60.2° in about 5° increments and a forward Mach number variation from 0.60 to 0.96.

SYMBOLS

B number of blades

b blade chord, ft

C_T thrust coefficient, $T/\rho n^2 D^4$

C_{T_W} thrust coefficient obtained from wake survey, $\int_{0.274}^{1.0} c_t \, dx$

c_l section lift coefficient, $\dfrac{\left\{\Delta p_t\right\}}{\frac{1}{2}\rho_t V^2} \dfrac{J}{B\frac{b}{D}\sqrt{1+\left(\frac{\pi x}{J}\right)^2}}$

c_t section thrust coefficient, $\frac{1}{4}\frac{J^2 \pi x \{\Delta p_t\}}{\frac{1}{2}\rho_t V^2}$

ΔC_T incremental thrust coefficient, difference between the instantaneous thrust coefficient of a tilted propeller and the thrust coefficient of an untilted propeller

D propeller diameter, ft

h blade section thickness, ft

J advance ratio, V/nD

M tunnel airstream Mach number

M_x helical section Mach number, $M\sqrt{1 + \left(\frac{\pi x}{J}\right)^2}$

M_t tip Mach number, $M\sqrt{1 + \left(\frac{\pi}{J}\right)^2}$

N propeller rotational speed, rpm

n propeller rotational speed, rps

P power, ft-lb/sec

$\{\Delta p_t\}$ time average of stagnation-pressure rise through the propeller

R propeller tip radius, ft

r radius to a blade element, ft

T thrust, lb

t time sec

V tunnel airstream velocity, ft/sec

x fractional radius to a propeller blade section, r/R

$\beta_{0.75R}$ blade-angle setting at 0.75 radial station, deg

ρ mass density of air, slugs/cu ft

ρ_t stagnation density, slugs/cu ft

ω angular velocity of propeller, deg/sec

APPARATUS AND METHODS

16-Foot Transonic Tunnel

This investigation was made in the Langley 16-foot transonic tunnel. A calibration of the slotted test section with the 6,000-horsepower propeller dynamometer installed is presented in reference 5. The Mach number range of the tunnel airstream with the dynamometer installed is from 0.20 to 0.96 and the Mach numbers quoted herein are accurate to ± 0.01. Figure 1 is a downstream view of the test section of the 16-foot transonic tunnel, showing the 6,000-horsepower propeller dynamometer and the Curtiss-Wright supersonic propeller (design no. 109622).

6,000-Horsepower Propeller Dynamometer

Two 3,000-horsepower induction motors are mounted in tandem on vertical support struts of circular-arc cross section. These two units are coupled together to provide a maximum of 8,000 horsepower for 5 minutes (overload) or 6,000 horsepower continuously (rated load). A detailed description of the 6,000-horsepower propeller dynamometer is given in reference 6. Spinner stresses limited the dynamometer rotational speed to 2,250 rpm during this investigation. The rotational speed of the dynamometer can be set to $\pm 1/4$ rpm.

Figure 2 is a sketch showing the dynamometer installed in the 16-foot transonic tunnel. A cylindrical fairing having the same diameter as the dynamometer and spinner extended from the minimum section of the tunnel throat to the forward spinner face. This body was installed to obtain approximately uniform axial and radial velocity in the plane of the propeller.

Propeller

The Curtiss-Wright supersonic propeller (design no. 109622) is 9.75 feet in diameter in the three-blade configuration. The propeller blades are solid steel and the airfoil sections are NACA 16-series symmetrical sections of 14-inch chord with a thickness distribution from 6 percent at the spinner to 2 percent at the propeller tip. The

blade-form curves are shown in figure 3. The propeller was designed for a Mach number of 0.95, a 35,000-foot altitude, and 2,600 rpm; these conditions result in an advance ratio of 2.2 and a design blade angle of approximately 45° at the 0.75 radial station.

Wake-Survey Rakes

Figure 2 shows the wake-survey rakes installed in the tunnel test section. The strut of the survey rake is made up of 8-percent-thick circular-arc airfoil sections with a constant 2-foot chord, and the probes extend 1 chord length ahead of the leading edge. The total-head probes and the orifices in the static-pressure probes were located 17 inches rearward of the center line of the propeller.

The major part of this investigation was completed with the survey rakes in position 2 as shown in figure 2(b). They were originally placed in position 1 but, as is explained subsequently, their angular position had to be changed to reduce the once-per-revolution, or 1-P, vibratory stresses.

TESTS AND REDUCTION OF DATA

Test Conditions

For most of this investigation, the tunnel Mach number was held constant, and the rotational speed of the dynamometer was varied to cover an advance-ratio range from a lightly loaded to a heavily loaded condition of the propeller. A small part of the investigation was run at a constant rotational speed of 1,600 rpm and the tunnel Mach number was varied to produce the desired J range; however, the Mach number of the runs at constant rotational speed was, in general, less than 0.60 and the data are not presented in this paper because they are believed to be of minor interest. The tunnel Mach number range was from 0.60 to 0.96 for blade angles from 45.4° to 60.2° set at the 0.75 radial station.

Tunnel-Flow Angularity

The presence of the dynamometer support strut and the wake survey rakes in the lower half of the tunnel test section created a blockage which caused some effective flow angularity and resulted in excessive 1-P stresses (as indicated by unpublished vibratory stress data). It was found that the vibratory bending stresses of the propeller could be reduced about one-half by moving the survey rakes from position 1 to position 2 as shown in figure 2(b).

Thrust Coefficient

The expression for the section thrust coefficient,

$$c_t = \frac{1}{4} \frac{J^2 \pi x \left\{p_t\right\}}{\frac{1}{2}\rho_t V^2}$$

has been derived in reference 7. The effects of drag, induced angle, and any rotational flow caused by strong shocks at supersonic Mach numbers have been neglected in this derivation. The variation of c_t with advance ratio was determined for each tube of the survey rake. The values of c_t were read at a particular J value and plotted against blade radius, and comparisons of these blade loadings were made for various Mach numbers. A typical data plot of the section thrust-coefficient distribution is shown in figure 4. The thrust grading curves were integrated to find C_{T_W} at each test point. In all cases, whether the survey rakes are in position 1 or 2, the integrated thrust coefficients and the blade loadings are the average of the data from both survey rakes even though, in general, the integrated data from rake B in position 2 would be in better agreement with force data.

Lift Coefficient

The expression for c_l from reference 7 is

$$c_l = \frac{\left\{\Delta p_t\right\}}{\frac{1}{2}\rho_t V^2} \frac{J}{B \frac{b}{D}\sqrt{1 + \left(\frac{\pi x}{J}\right)^2}}$$

As before, the total-head tube measures $\left\{\Delta p_t\right\}$ directly and the rest of the equation comes from easily measured quantities.

RESULTS AND DISCUSSION

Effect of Tunnel-Flow Angularity on a Comparison of Integrated Thrust Coefficients With Force Data

The presence of an effective tunnel-flow angularity was indicated by excessive blade vibratory-bending stresses with the survey rakes in position 1. Unpublished stress data show that these 1-P stresses were reduced approximately one-half when the survey rakes were moved to position 2. Reference 8 indicates that unless the survey rakes are diametrically opposed, large errors can be introduced when using wake surveys obtained where tunnel-flow angularity exists. An attempt is made to explain the effect of flow angularity by applying the theory of pitched propellers to the data presented herein.

Figure 5 shows a theoretical variation of ΔC_T with ωt, where ωt is taken as zero when the blade is vertically upward and the propeller thrust axis is at a positive angle of attack (see ref. 9). The solid curve in figure 5 shows a variation of ΔC_T which was calculated by assuming a thrust-axis angle of inclination of 0.8° or an effective flow angularity of 0.8°. By taking the difference between the integrated thrust coefficients for the individual survey rakes and the thrust coefficient obtained from force data, a value of incremental thrust coefficient can be found for the individual survey rakes A and B. The diamond symbols in figure 5 show these incremental thrust coefficients when the survey rakes are in position 1, separated by 135°. (Data for $M = 0.60$, $J = 3.8$, and $\beta_{0.75R} = 60.2^\circ$ are typical of the analyses made for all the data.) These points are in good agreement with the theoretical curve, and it is indicated that an average of the data from the two survey rakes should be nearly equal to force data. This is the expected result from two survey rakes almost diametrically opposed when the downgoing blade is experiencing an increased angle of attack and the other blades are at a decreased angle of attack. Data were not obtained above a Mach number of 0.60 with the survey rakes in position 1 because of excessive 1XP bending stresses.

As explained previously, the effective flow angularity was reduced about one-half when the survey rakes were moved to position 2. For this reason the dashed curve in figure 5 was calculated by assuming a flow angularity of 0.4°. The incremental thrust coefficients obtained from survey rakes A and B in position 2 are plotted in figure 5 for the assumed location of $\omega t = 0^\circ$, and both values are higher than force data. A satisfactory explanation for this discrepancy has not been found; however, if it is assumed that the proximity of the survey rakes in position 2 created a small local blockage, then the propeller blade would experience

a small local increase in angle of attack and the thrust coefficients measured by the survey rakes would be high. Another possible explanation would be a change in the direction of the effective flow angle when the survey rakes were moved from position 1 to position 2.

Figure 6 shows the thrust loadings for rakes A and B in both positions and indicates the variation of thrust around the propeller disk which produced the results shown by the data points in figure 5. Figure 6 indicates that in position 1 the thrust loading from rake A is lower that that from rake B, while in position 2 the opposite result is obtained.

Figure 7 shows the comparison of the integrated thrust coefficients with the force data from reference 5 for blade angles of 50.8°, 54.7°, and 60.2° up to a Mach number of 0.93. The theoretical curve (solid line) in figure 5 indicates that the average of the data from the two survey rakes in position 1 would be in good agreement with the thrust coefficients from force data, and figure 7(a) shows that C_{T_W} is in excellent agreement with the force data for $\beta_{0.75R} = 50.8°$ and 60.2°.

When the survey rakes are in position 2, figure 7 indicates that, in general, the integrated thrust coefficients are increased by 0 to 13 percent over the force data.

Thrust Loading at Constant Advance Ratios

The variation of thrust loading with Mach number at constant advance ratios for blade angles of 45.4°, 50.8°, 54.7°, and 60.2° is shown in figure 8. Figure 9 shows the variation of the integrated thrust coefficient with Mach number for blade angles of 50.8°, 54.7°, and 60.2° and a comparison with force data. The advance ratios chosen are near the value for maximum efficiency at a Mach number of 0.70.

Advance ratio of 2.24.- When the blade angle is set at 45.4°, the advance-ratio range is limited by the maximum propeller rotational speed at Mach numbers above 0.70. Figure 8(a) indicates that the thrust loading increases when the Mach number is increased from 0.60 to 0.70, with the maximum value of section thrust coefficient occurring near $x = 0.82$.

Advance ratio of 2.75.- Figure 8(b) shows that the thrust loading increases at all blade stations up to a Mach number of 0.80 at $J = 2.75$. The values of section thrust coefficient continue to increase over the outboard stations ($x > 0.70$) when the Mach number is increased to 0.84 and 0.89, but some reduction occurs near $x = 0.60$ where the local section Mach number is approximately 1.0. The integrated thrust coefficient

increases with Mach number up to 0.85 and there is a slight decrease as the Mach number is increased to 0.89 as shown in figure 9. It should be noted that the combination of a Mach number of 0.89 and maximum propeller rotational speed produces supersonic section speeds outboard of $x = 0.45$ with a tip Mach number of 1.35, but no severe compressibility losses are noted at any section and the thrust coefficient has decreased very slightly above a forward Mach number of 0.85.

Advance ratio of 3.10.- The thrust loadings for Mach numbers up to 0.96 at $J = 3.10$ and a blade angle of 54.7° are shown in figure 8(c). The section thrust coefficients increase smoothly to a Mach number of 0.80 and the integrated thrust coefficient reaches a maximum at a Mach number of 0.83 (fig. 9). When the Mach number is increased to 0.96, the thrust-coefficient decrease can be directly attributed to the losses in section thrust coefficient, with the greater percentage losses occurring inboard of $x = 0.80$. At Mach numbers up to 0.89 the section velocities are lower for the 54.7° blade angle and $J = 3.10$ than for the 50.8° blade angle and $J = 2.75$: however, the angle-of-attack distribution along the blade is less favorable at the higher advance ratio, and losses are shown over the inboard sections where the angle of attack is increased.

Advance ratio of 3.90.- The effects of Mach number on the section thrust coefficients at a 60.2° blade angle are similar to those for a 54.7° blade angle up to a Mach number of 0.80, but the losses are more severe when the Mach number is increased to 0.96. Figure 9 indicates that C_{T_W} reached a maximum at a Mach number of 0.82 for the 60.2° blade-angle setting. In general, the losses in section thrust coefficient are shown to be more severe for the higher blade angles and advance ratios.

Thrust Loading at Advance Ratios for Maximum Efficiency

The variation of section thrust-coefficient distribution with Mach number for blade angles of 50.8°, 54.7°, and 60.2° is shown in figure 10 at advance ratios for maximum efficiency obtained from reference 5. The thrust loading at a 50.8° blade angle for Mach numbers from 0.60 to 0.80 is shown in figure 10(a). The thrust loading increases with an increase in Mach number from 0.60 to 0.70, and the peak remains approximately the same when the Mach number is increased to 0.80 but is shifted slightly inboard.

Figure 10(b) shows the section thrust-coefficient distribution for Mach numbers from 0.60 to 0.89 at advance ratios for maximum efficiency and $\beta_{0.75R} = 54.7°$. There is an increase in thrust loading as the Mach number is increased from 0.60 to 0.80 and the loading remains almost constant when the Mach number is increased to 0.89. The advance ratio was

not decreased sufficiently to obtain maximum efficiency at Mach numbers of 0.93 and 0.96.

Thrust loadings at $\beta_{0.75R} = 60.2^\circ$ for the Mach number range and advance ratios for maximum efficiency are shown in figure 10(c). The trend of the data indicates that the advance ratio and blade angle would have to decrease toward the design condition (advance ratio of 2.2 and about 45° blade angle) in order to obtain optimum efficiency.

Lift-Coefficient Distribution

The lift-coefficient distribution over the blade radius at $\beta_{0.75R} = 54.7^\circ$ for a Mach number range from 0.60 to 0.96 at $J = 3.10$ is shown in figure 11(a). Section lift coefficients along the blade radius are shown in figure 11(b) at advance ratios for maximum efficiency and Mach numbers from 0.60 to 0.89. There is a general increase in section lift-coefficient values when the Mach number is increased from 0.60 to 0.80, and the location of the maximum value remains near $x = 0.70$ for both the loadings at constant advance ratio and the loadings at the advance ratios for maximum efficiency. The effects of compressibility are shown in figure 11(a) by the decrease in section lift coefficient above a Mach number of 0.80, the greatest percentage decrease generally occurring inboard of $x = 0.75$. These small effects are noted in the regions where the local speeds are near a Mach number of 1.0 when the forward Mach number is 0.89 and above.

CONCLUDING REMARKS

An investigation has been made to determine the thrust and thrust loading by wake surveys of the total pressure in the slipstream of a supersonic-type three-blade propeller. The Mach number range was from 0.60 to 0.96 for blade-angle settings from 45.4° to 60.2° at the 0.75 radial station.

The results of the investigation indicate that the integrated thrust-coefficient values are in good agreement with the force data. Operation at Mach numbers up to 0.89 at a blade angle of 50.8° and an advance ratio of 2.75 produced no severe compressibility losses in thrust loading, and the thrust coefficient decreased very slightly above a forward Mach number of 0.85. The losses in section thrust coefficient were more severe for the higher blade angles and advance ratios. The trend of the data

indicates that the advance ratio and blade angle would have to decrease toward the design condition (advance ratio of 2.2 and about 45° blade angle) in order to obtain optimum efficiency.

Langley Aeronautical Laboratory,
National Advisory Committee for Aeronautics,
Langley Field, Va., August 20, 1953.

REFERENCES

1. Maynard, Julian D., and Steinberg, Seymour: The Effect of Blade-Section Thickness Ratios on the Aerodynamic Characteristics of Related Full-Scale Propellers at Mach Numbers up to 0.65. NACA RM L9D29, 1949.

2. Delano, James B., and Carmel, Melvin M.: Investigation of NACA 4-(0)(03)-045 and NACA 4-(0)(08)-045 Two-Blade Propellers at Forward Mach Numbers to 0.925. NACA RM L9L06a, 1950.

3. Igoe, William B., and Davidson, Robert E.: Propeller Induced Angles of Attack and Section Angles of Attack for the NACA 10-(3)(066)-03 10-(3)(049)-03, 10-(3)(090)-03, 10-(5)(066)-03, and 10-(0)(066)-03 Propellers. NACA RM L51L06, 1952.

4. Harrison, Daniel E., and Milillo, Joseph R.: The Effect of Thickness Ratio on Section Thrust Distribution As Determined From a Study of Wake Surveys of the NACA 4-(0)(03)-045 and 4-(0)(08)-045 Two-Blade Propellers up to Forward Mach Numbers of 0.925. NACA RM L51B05, 1951.

5. Evans, Albert J., and Liner, George: A Wind-Tunnel Investigation of the Aerodynamic Characteristics of a Full-Scale Supersonic-Type Three-Blade Propeller at Mach Numbers to 0.96. NACA RM L53F01, 1953.

6. Wood, John H., and Swihart, John M.: The Effect of Blade-Section Camber on the Static Characteristics of Three NACA Propellers. NACA RM L51L28, 1952.

7. Davidson, Robert E.: Propeller Lift and Thrust Distribution From Wake Surveys of Stagnation Conditions. NACA RM L51K29, 1952.

8. Pendley, Robert E.: Effect of Propeller-Axis Angle of Attack on Thrust Distribution Over the Propeller Disk in Relation to Wake-Survey Measurement of Thrust. NACA WR L-517, 1945. (Formerly NACA ARR L5J02b.)

9. Crigler, John L., and Gilman, Jean, Jr.: Calculation of Aerodynamic Forces on a Propeller in Pitch or Yaw. NACA TN 2585, 1952. (Supersedes NACA RM L8K26.)

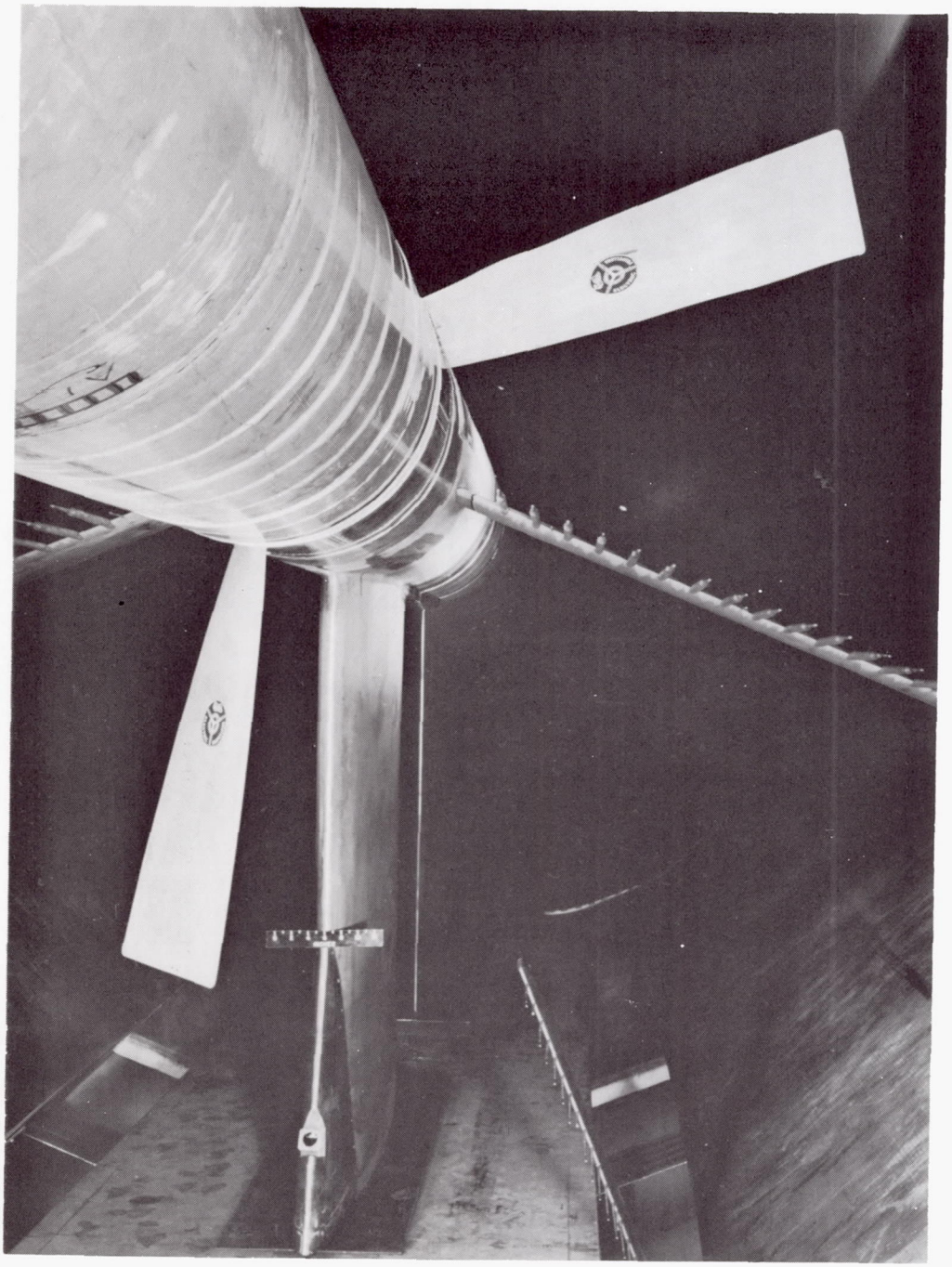

L-75372

Figure 1.- Downstream view of the 6,000-horsepower dynamometer and survey-rake assembly in the test section of the 16-foot transonic tunnel.

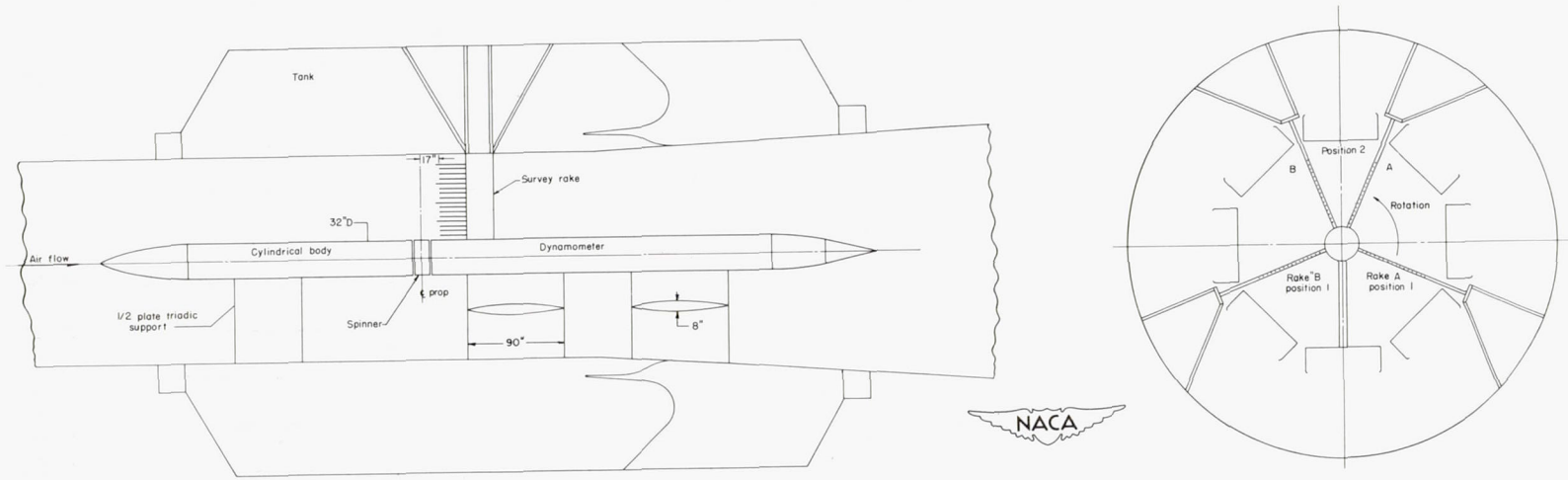

(a) Cross section.

(b) Downstream view.

Figure 2.- Dynamometer and survey-rake installation in the test section of the 16-foot transonic tunnel.

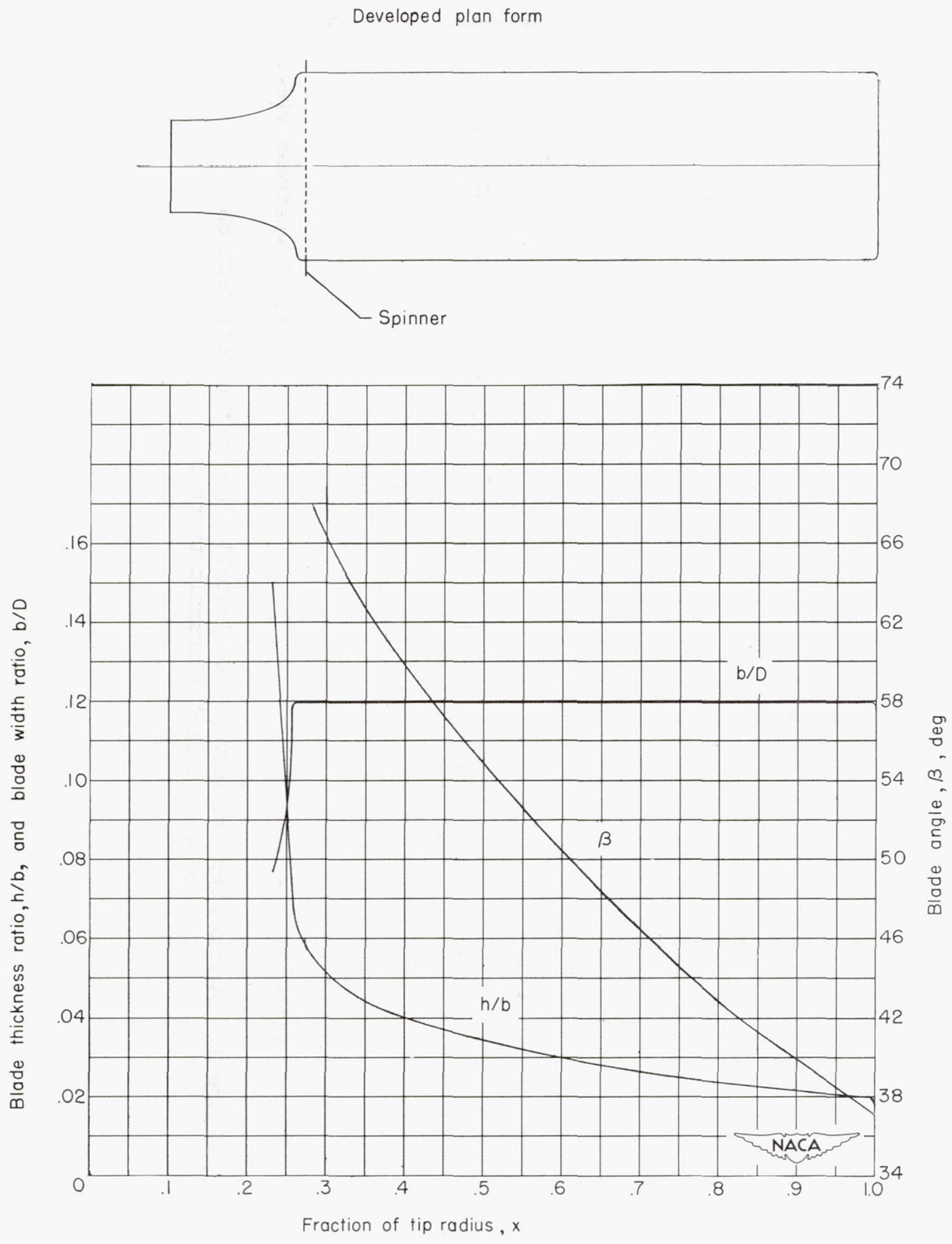

Figure 3.- Blade-form characteristics of the Curtiss-Wright supersonic propeller (design no. 109622).

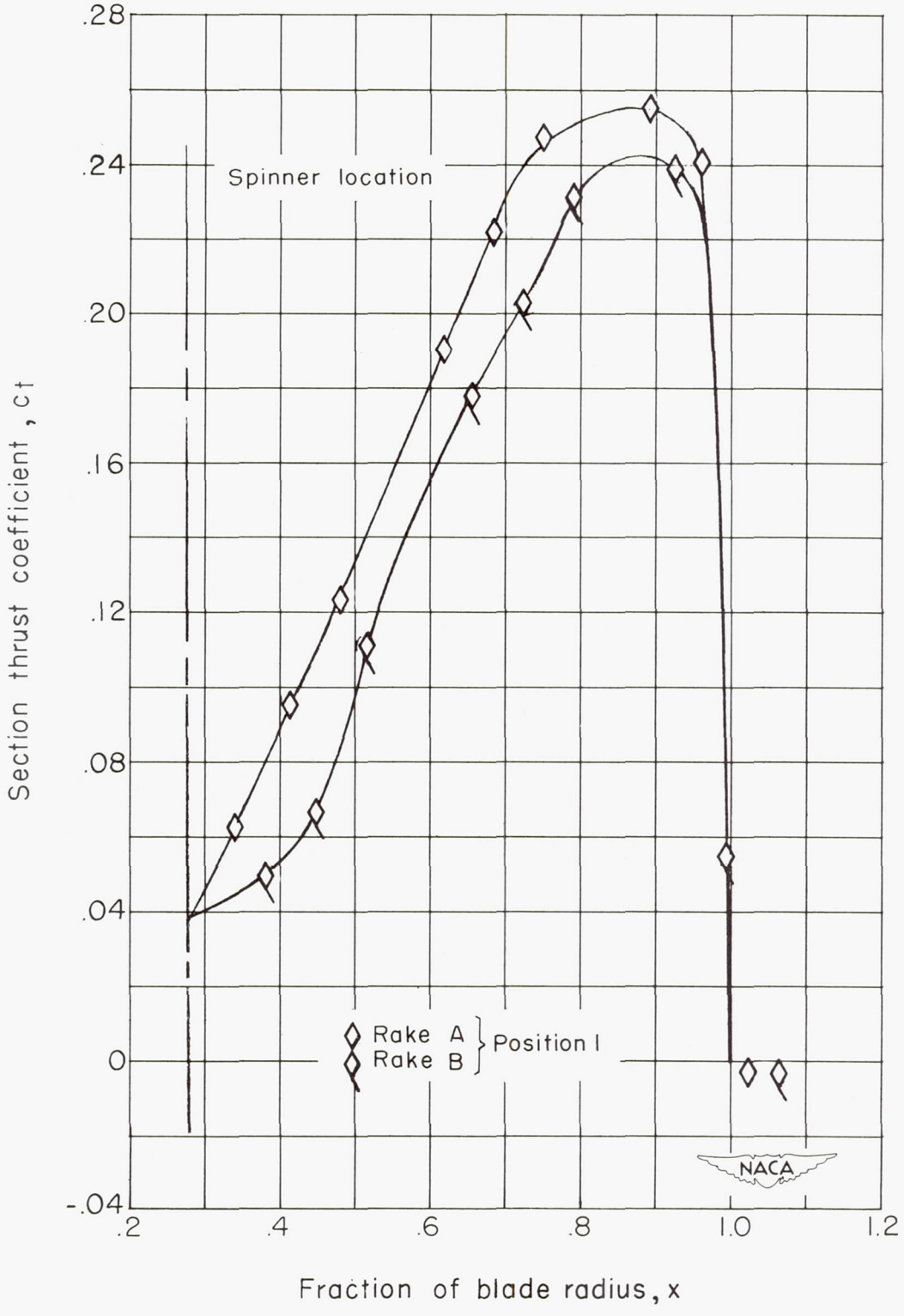

Figure 4.- A typical data plot of the section thrust coefficient. $M = 0.60$; $\beta_{0.75R} = 50.8^{\circ}$; $J = 2.552$.

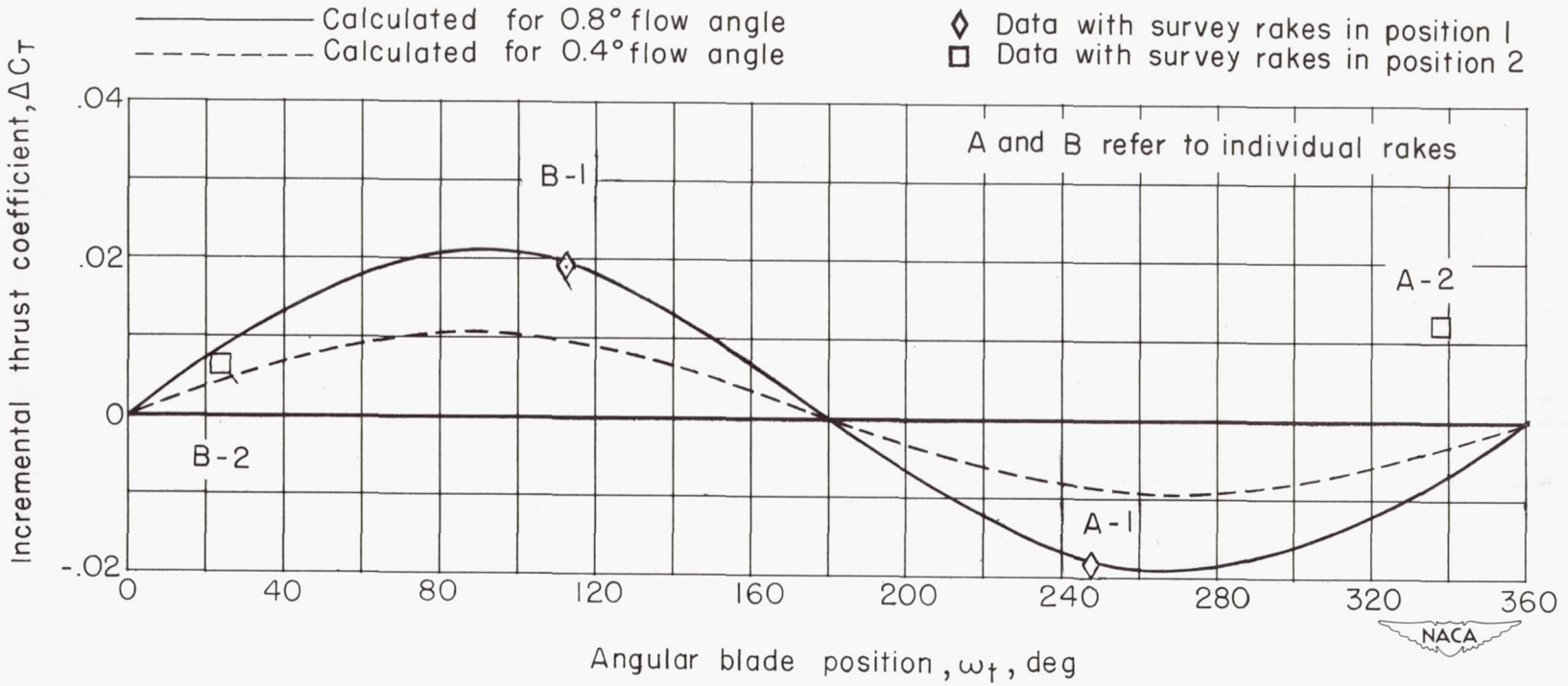

Figure 5.- Variation of incremental thrust coefficient with angular blade position. Data points are the differences between integrated thrust coefficients for the individual survey rakes and the force data at $M = 0.60$, $J = 3.8$, and $\beta_{0.75R} = 60.2^{\circ}$.

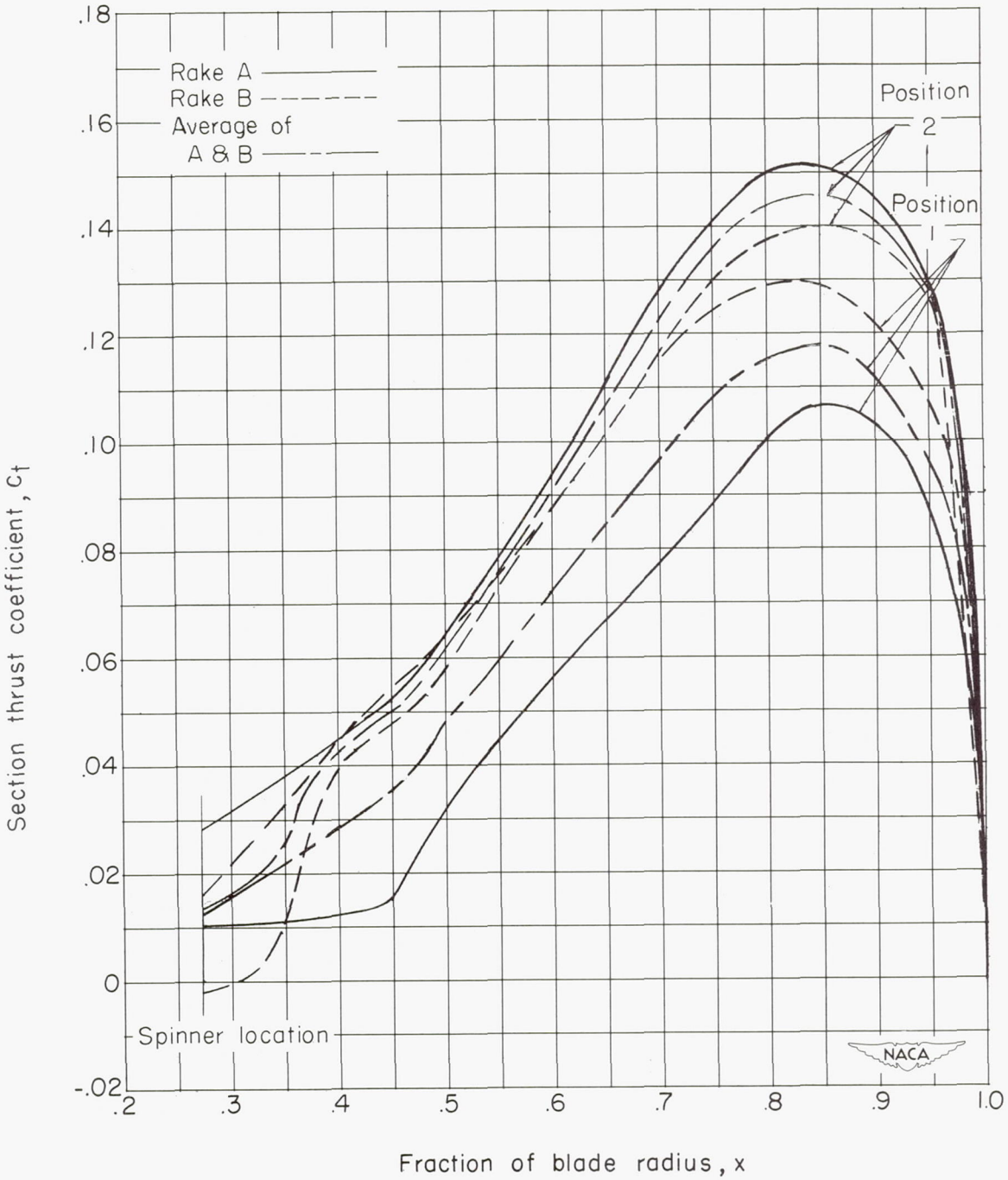

Figure 6.- The thrust loading from the two survey rakes A and B in positions 1 and 2 at $\beta_{0.75R} = 50.8^{\circ}$, M = 0.60, and J = 2.725.

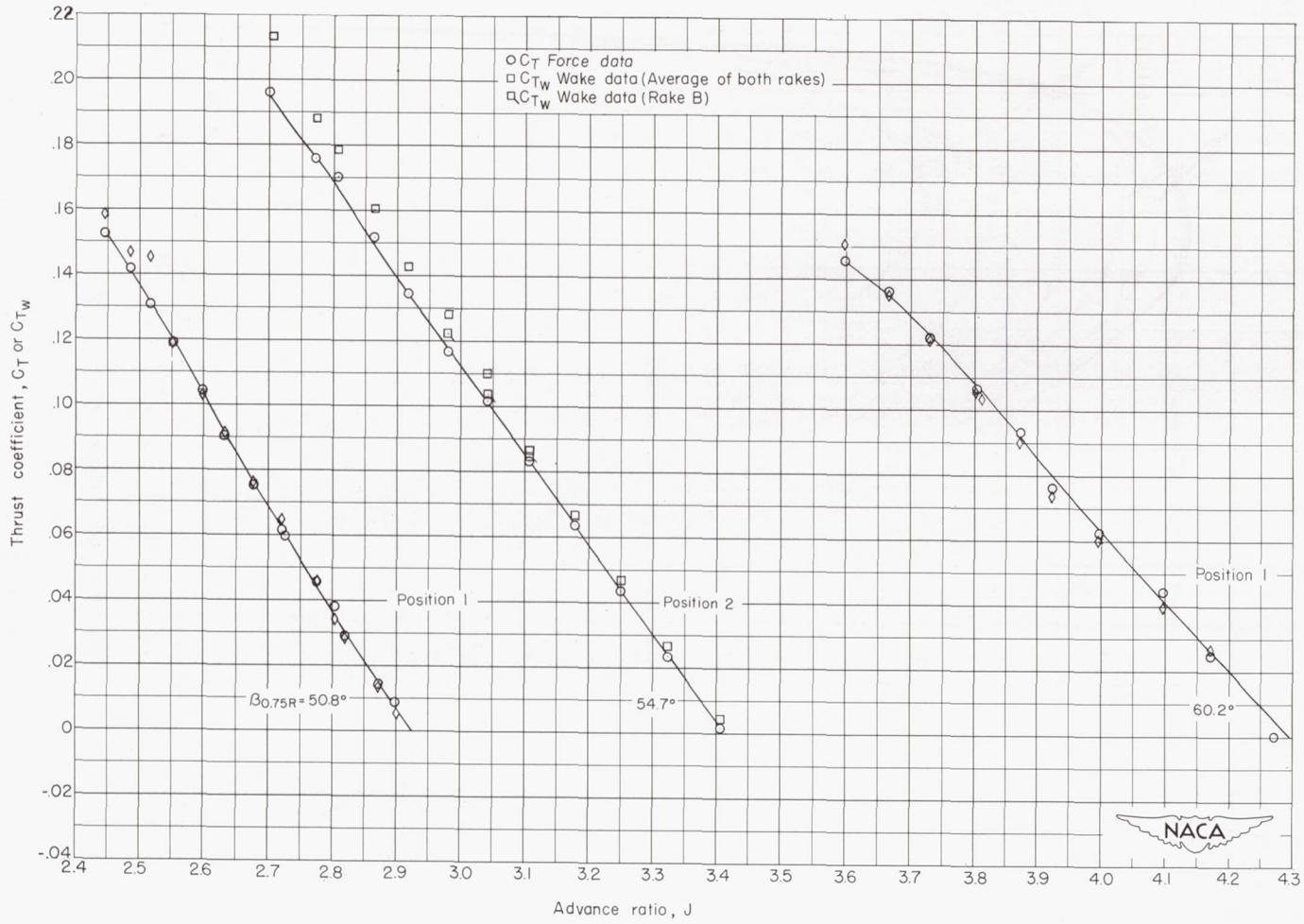

(a) M = 0.60.

Figure 7.- Comparison of the variation of the integrated thrust coefficient and the force-test thrust coefficient with advance ratio J.

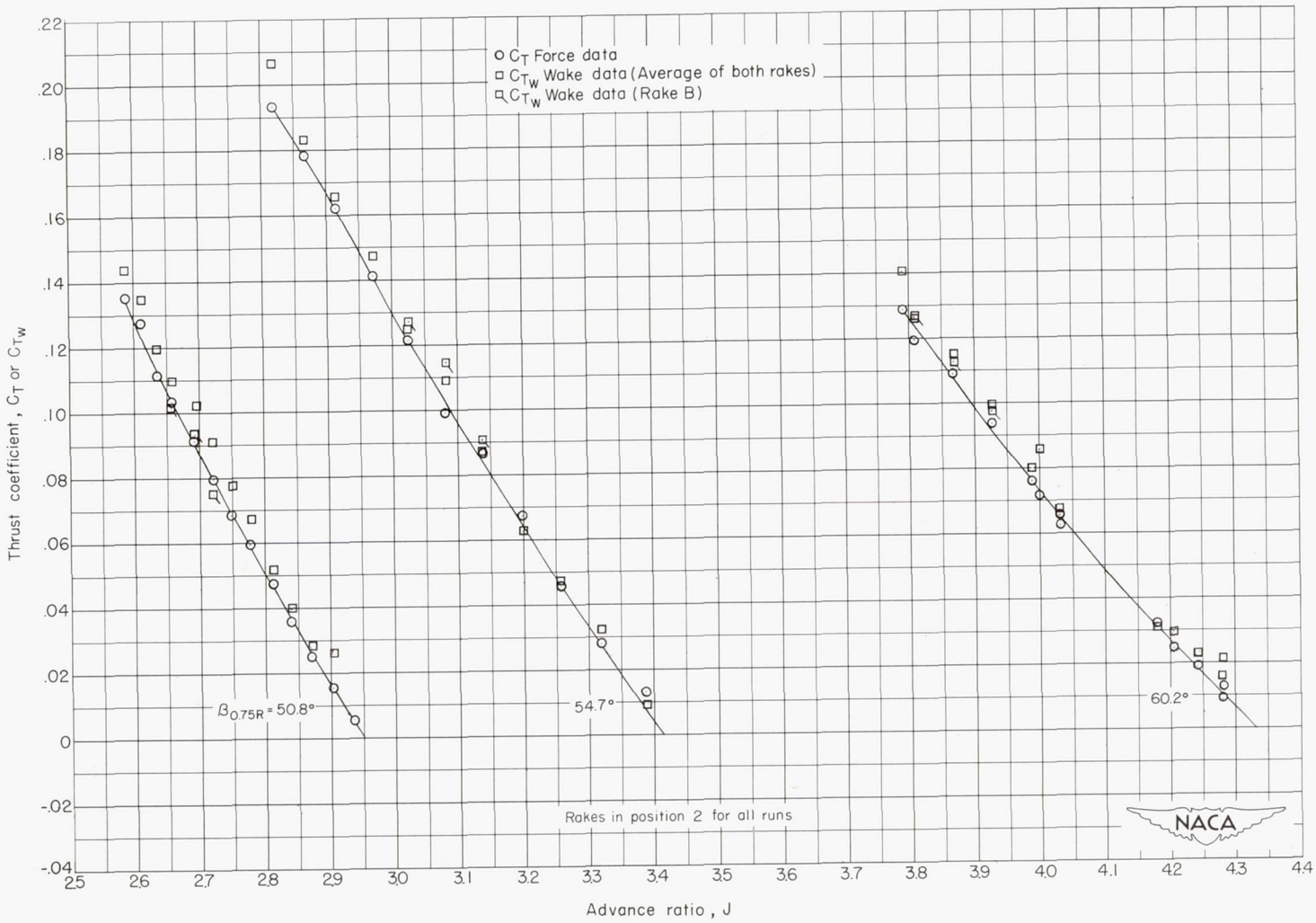

(b) M = 0.70.

Figure 7.- Continued.

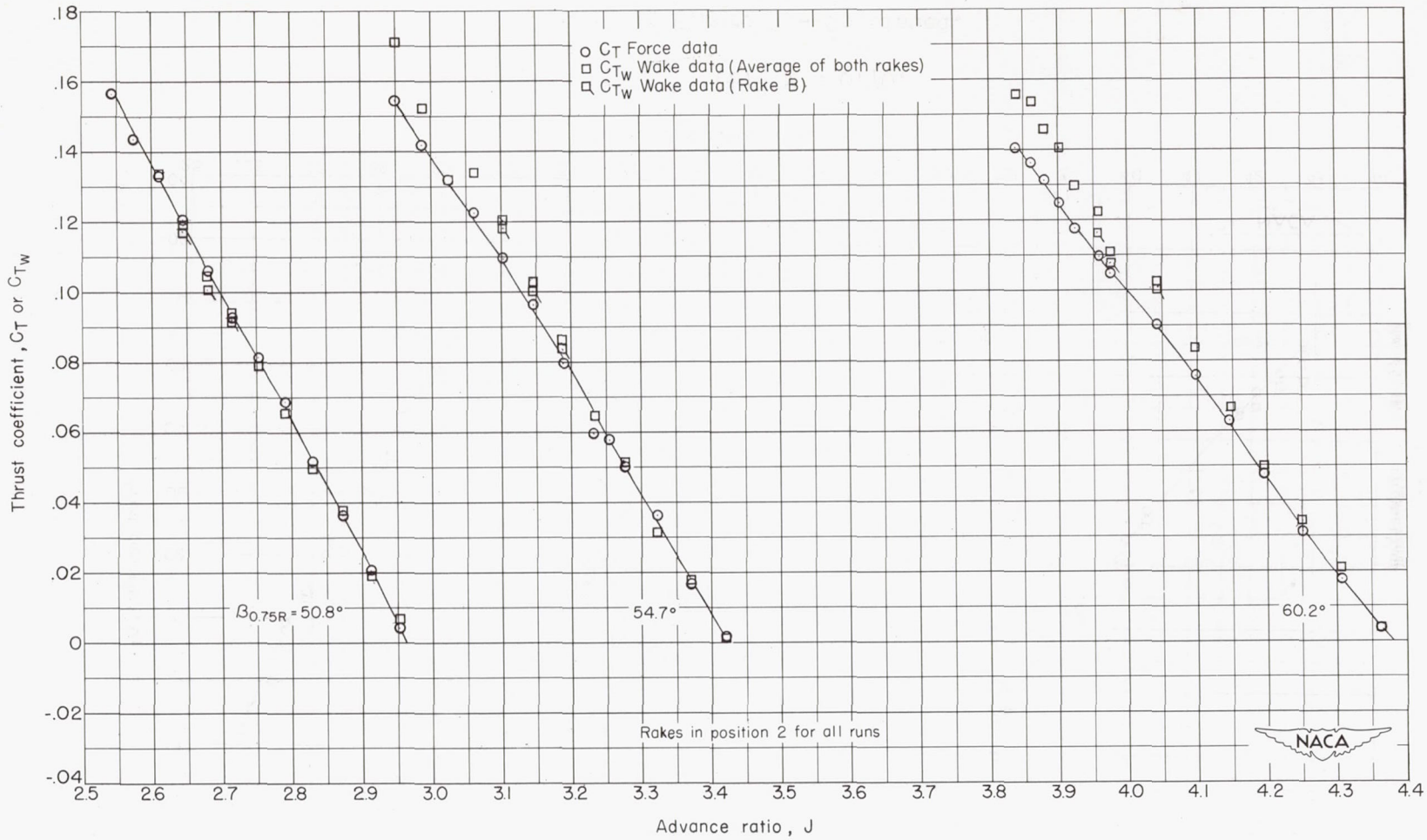

(c) M = 0.80.

Figure 7.- Continued.

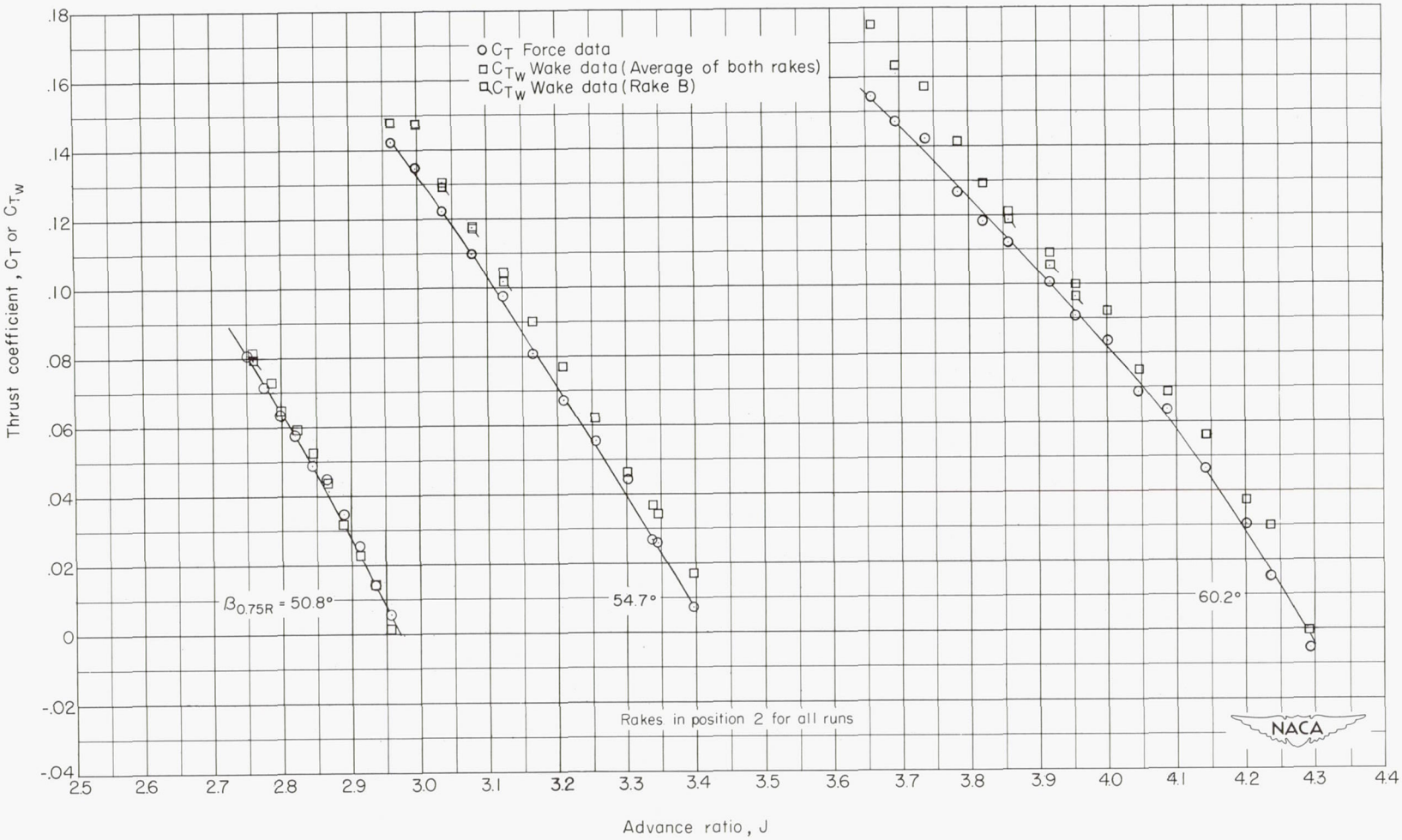

(d) M = 0.89.

Figure 7.- Continued.

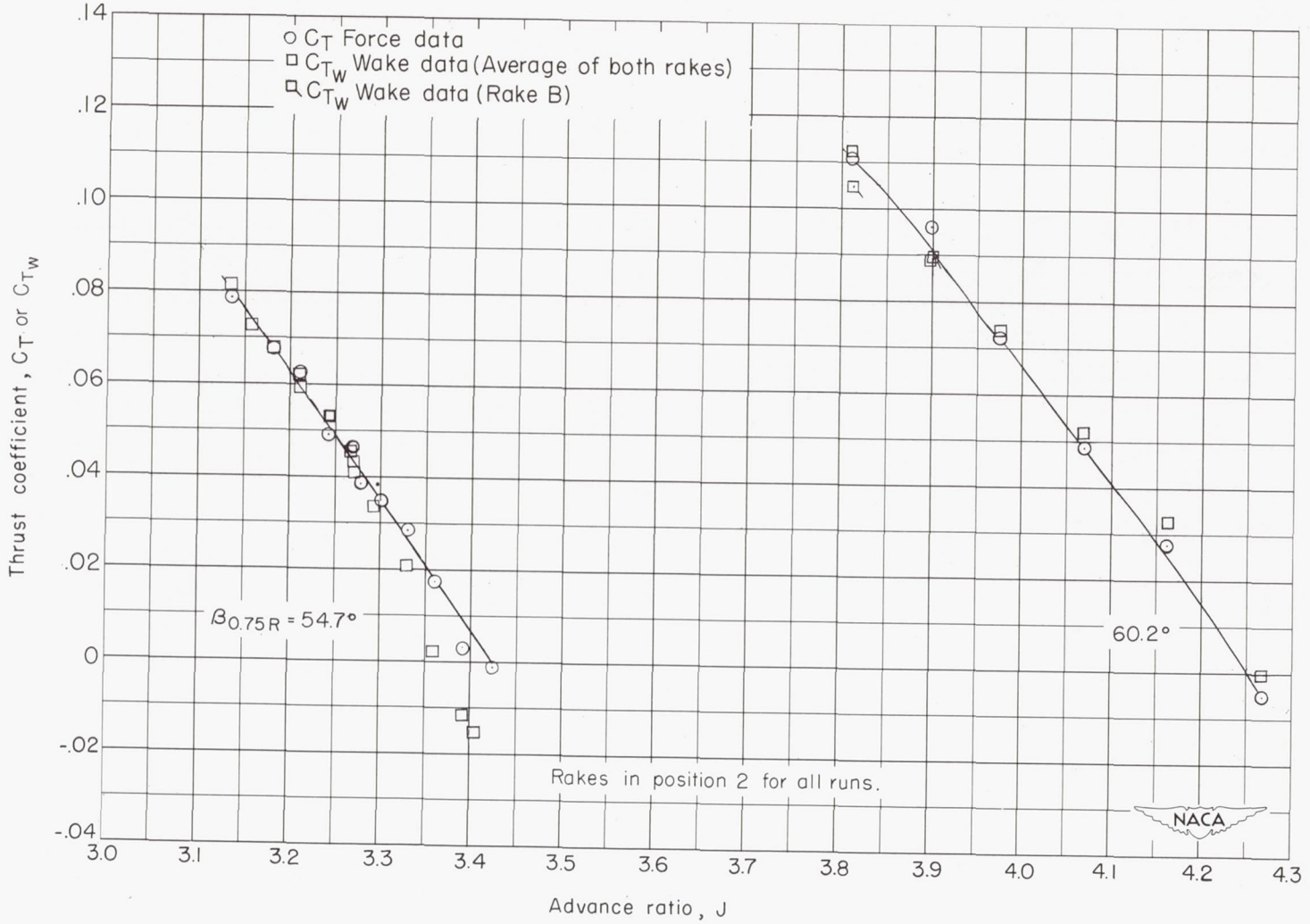

(e) M = 0.93.

Figure 7.- Concluded.

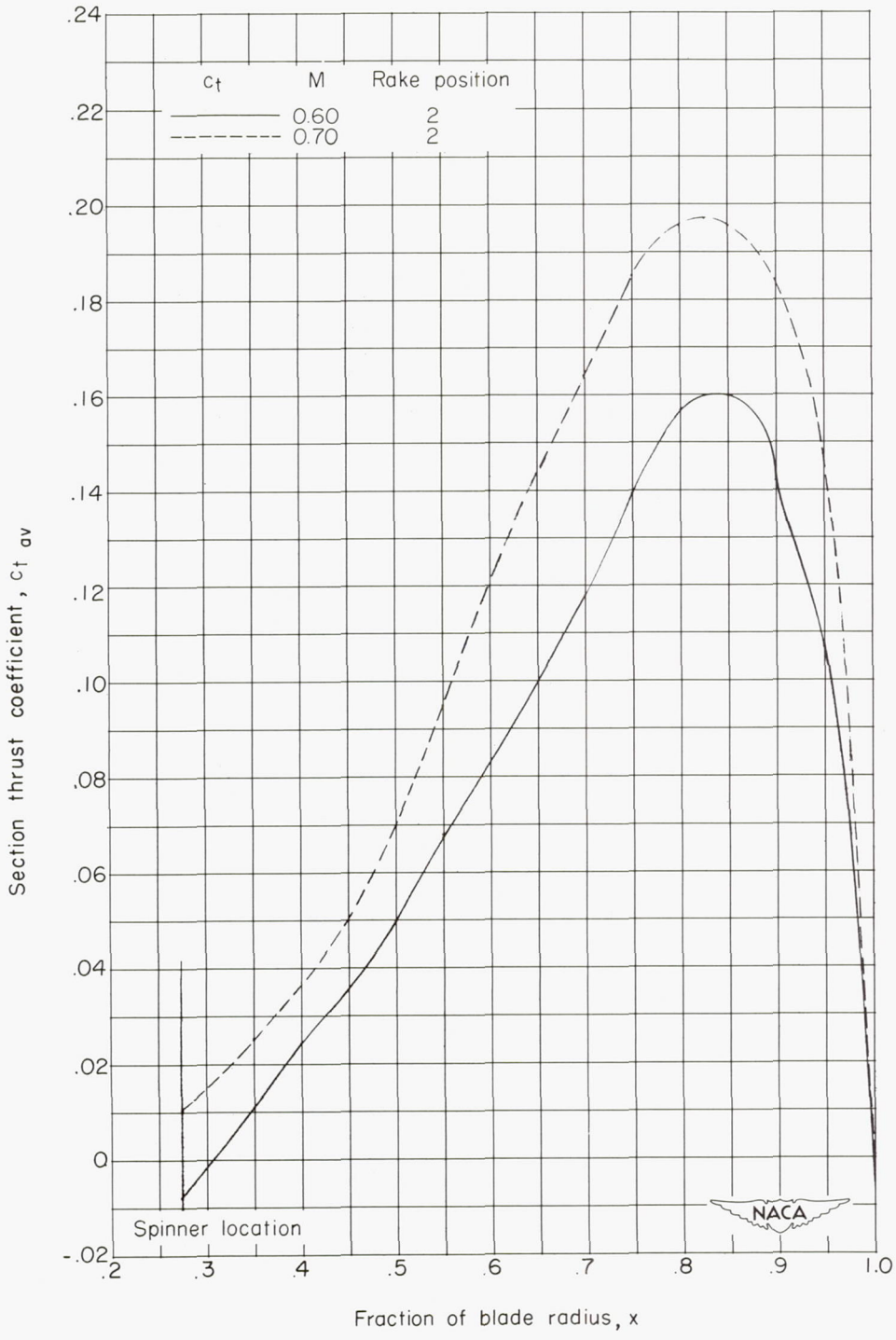

(a) $\beta_{0.75R} = 45.4^{\circ}$; J = 2.24.

Figure 8.- The thrust-loading variation with Mach number for constant advance ratio.

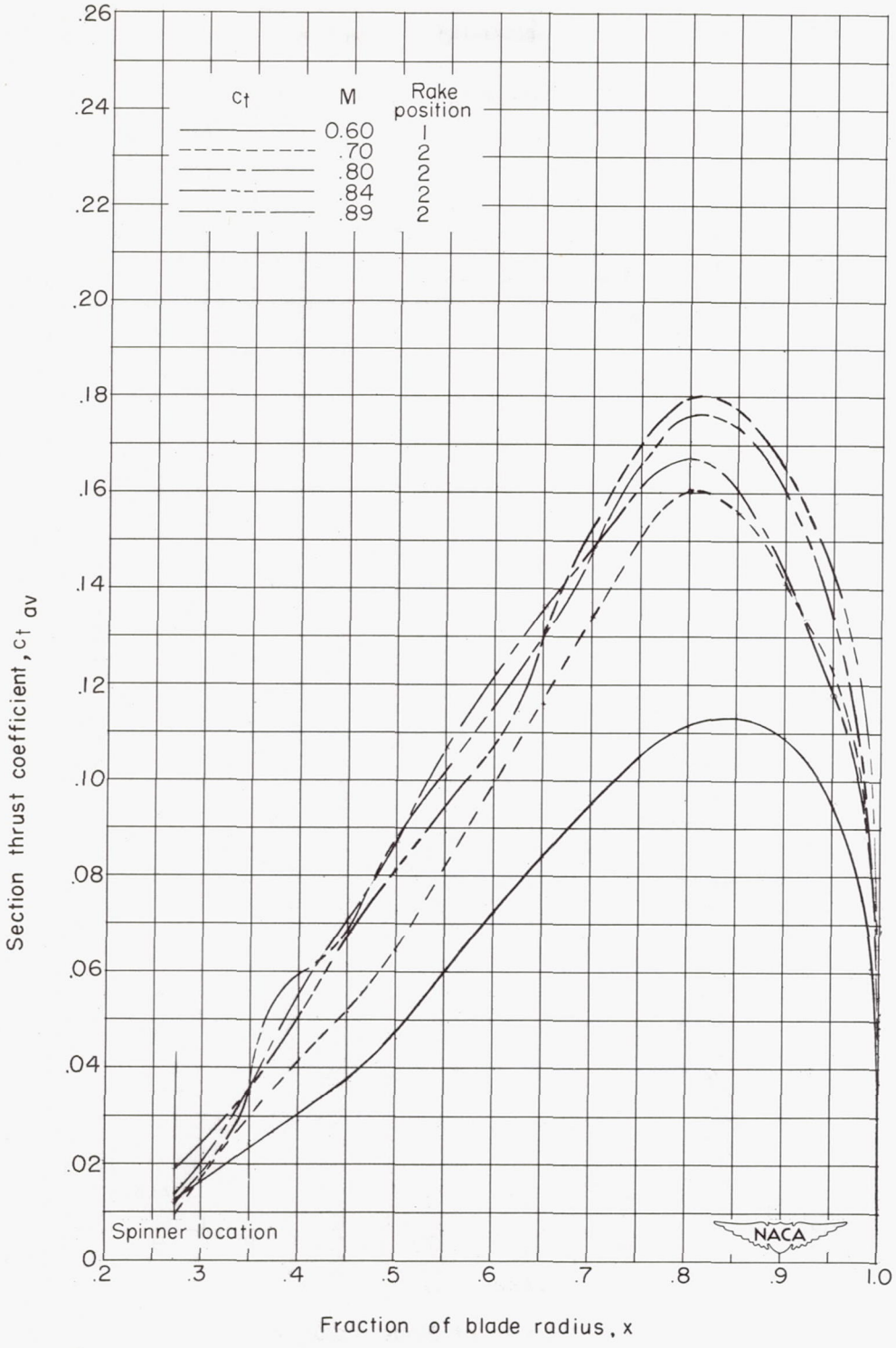

(b) $\beta_{0.75R} = 50.8^{\circ}$; J = 2.75.

Figure 8.- Continued.

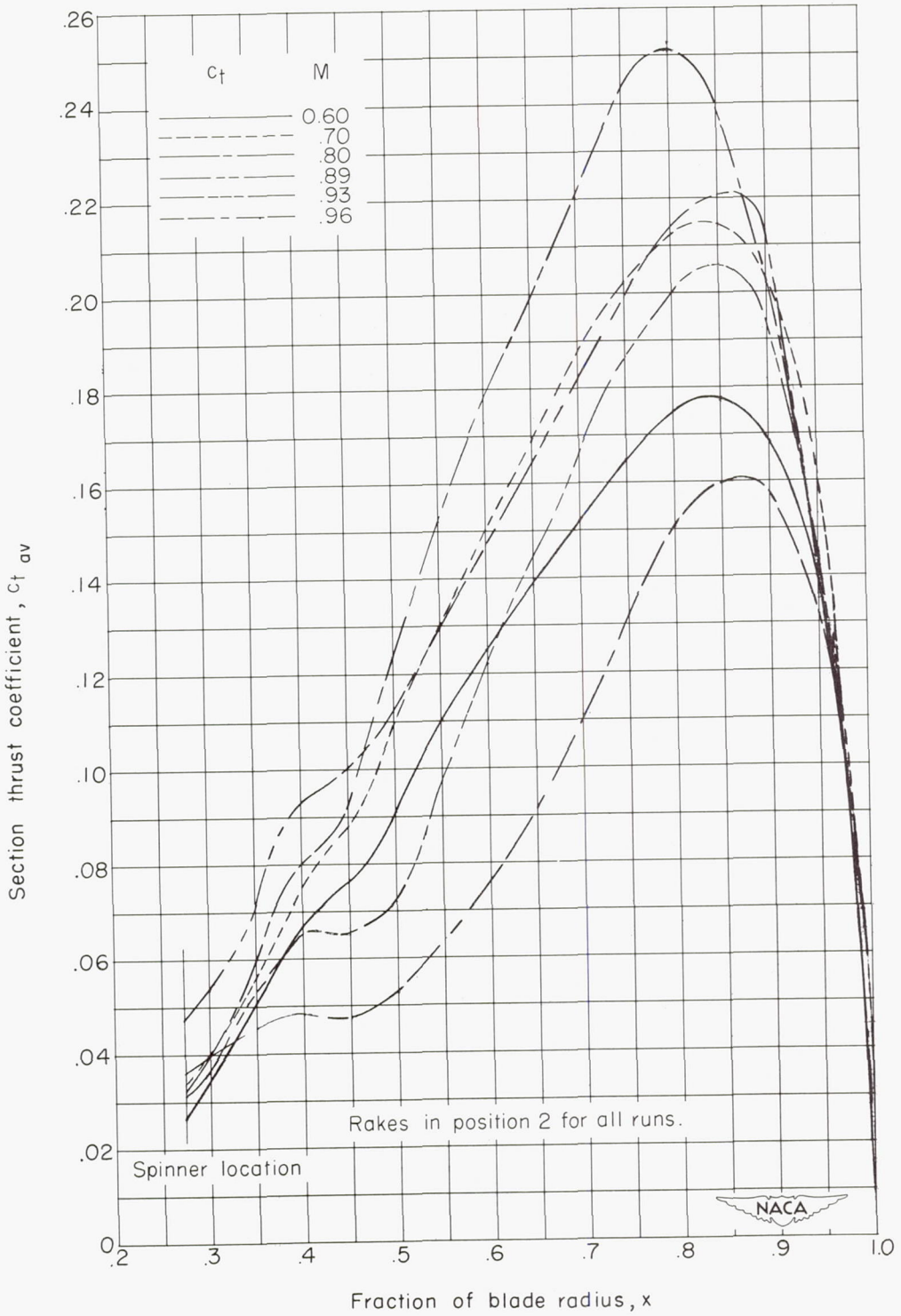

(c) $\beta_{0.75R} = 54.7^{\circ}$; J = 3.10.

Figure 8.- Continued.

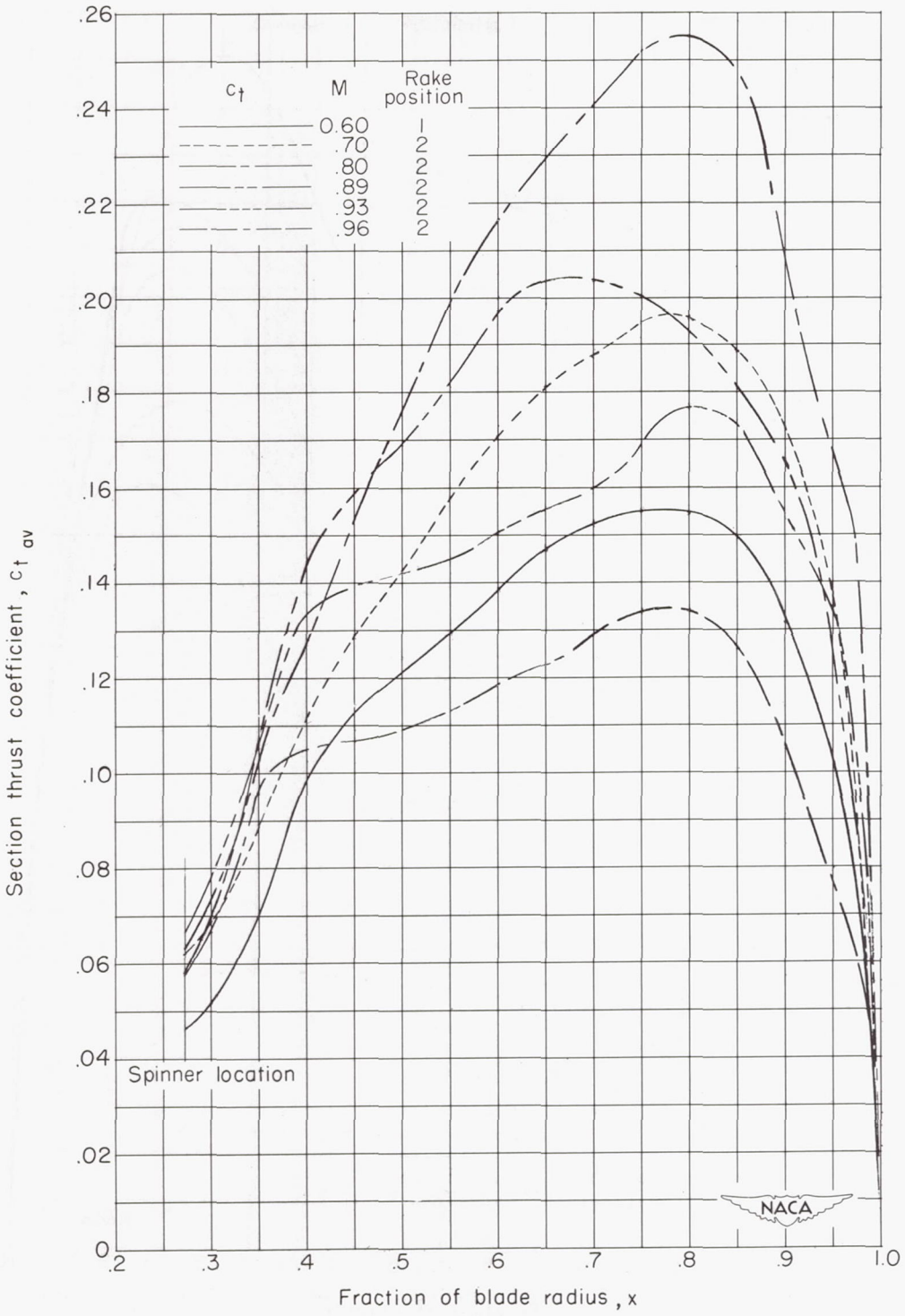

(d) $\beta_{0.75R} = 60.2^{\circ}$; J = 3.90.

Figure 8.- Concluded.

CONFIDENTIAL

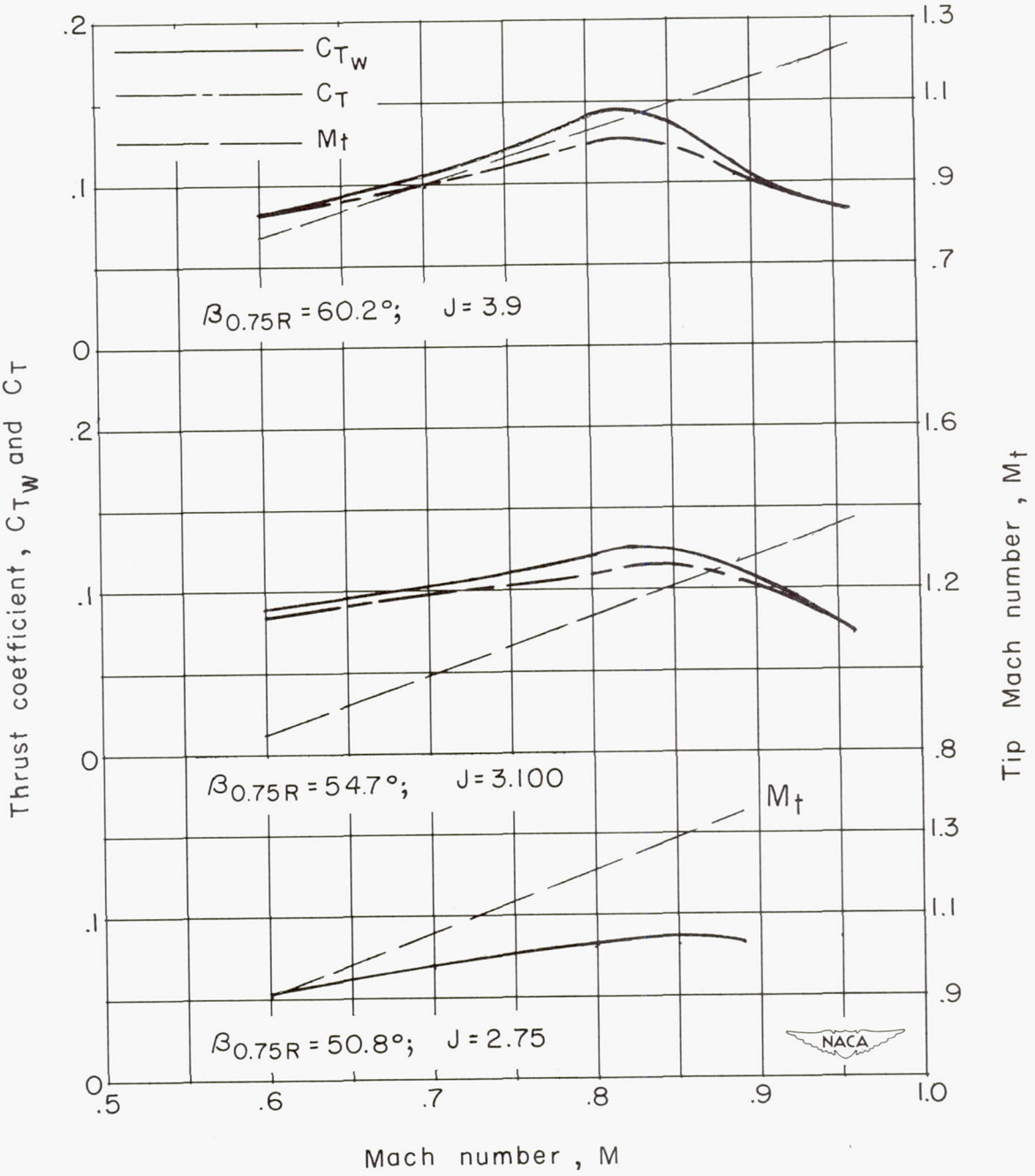

Figure 9.- Variation of thrust coefficient and tip Mach number with free-stream Mach number for several blade angles and advance ratios.

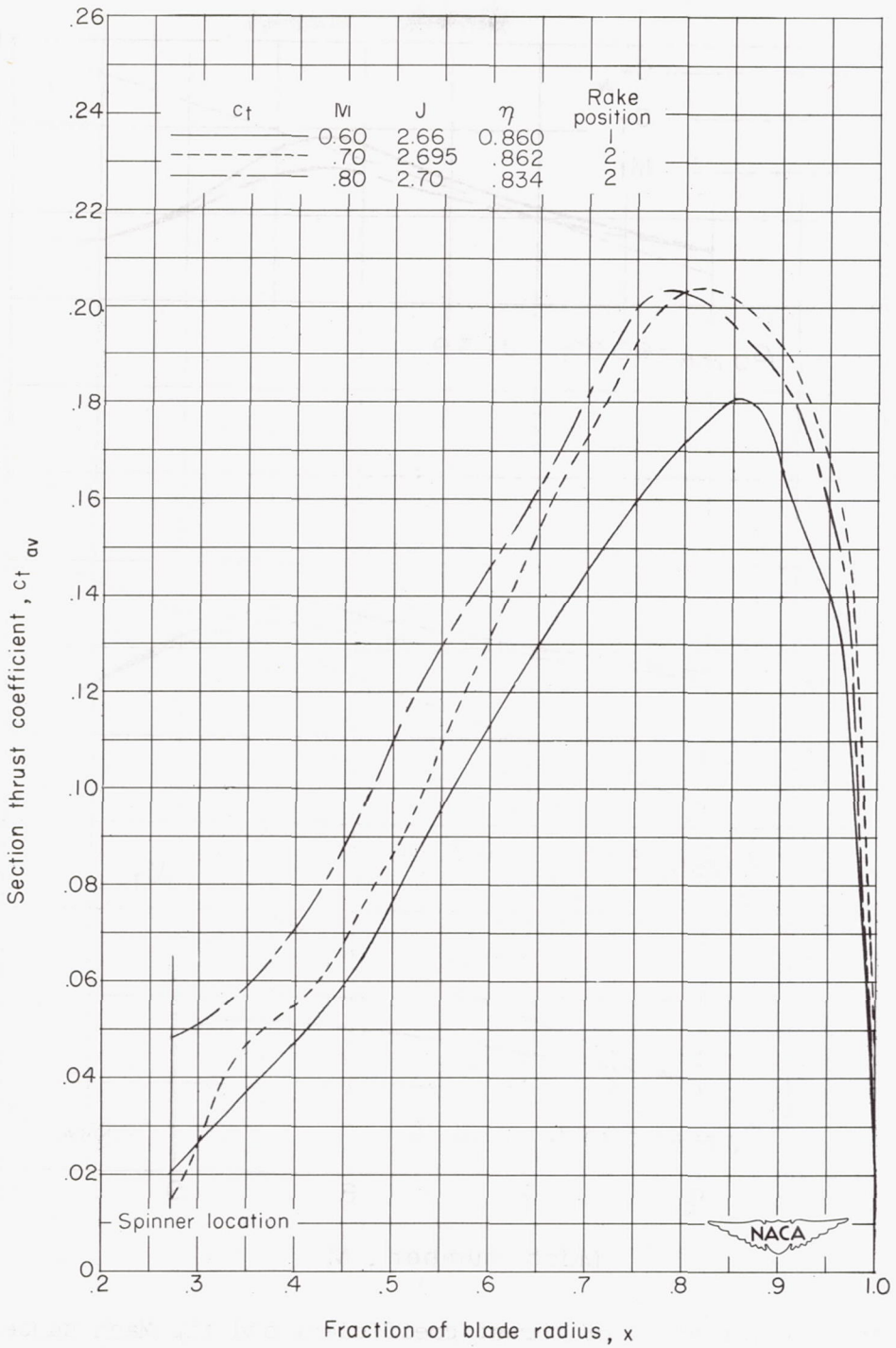

(a) $\beta_{0.75R} = 50.8^{\circ}$.

Figure 10.- Thrust-loading variation with Mach number at advance ratios for maximum efficiency.

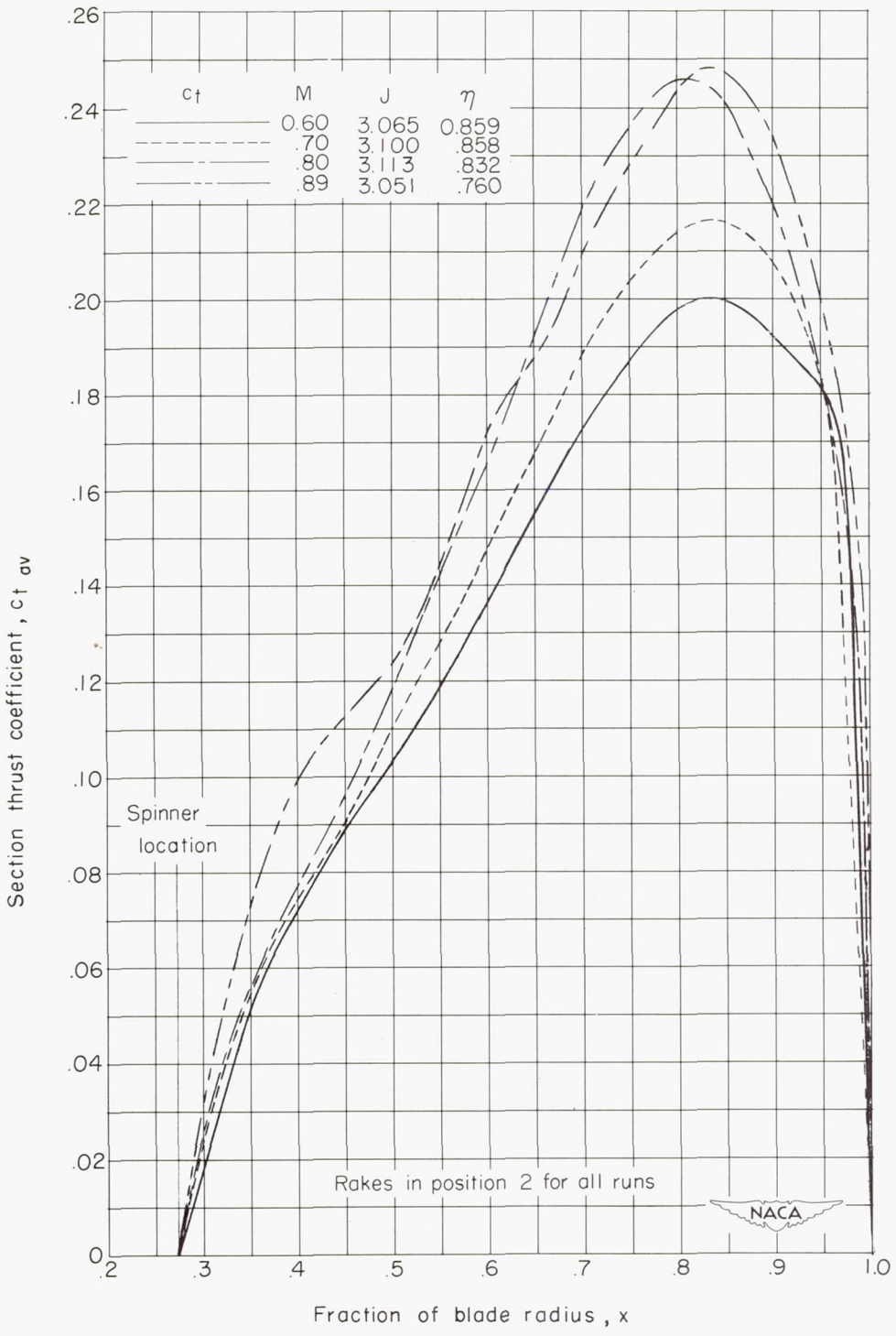

(b) $\beta_{0.75R} = 54.7^{\circ}$.

Figure 10.- Continued.

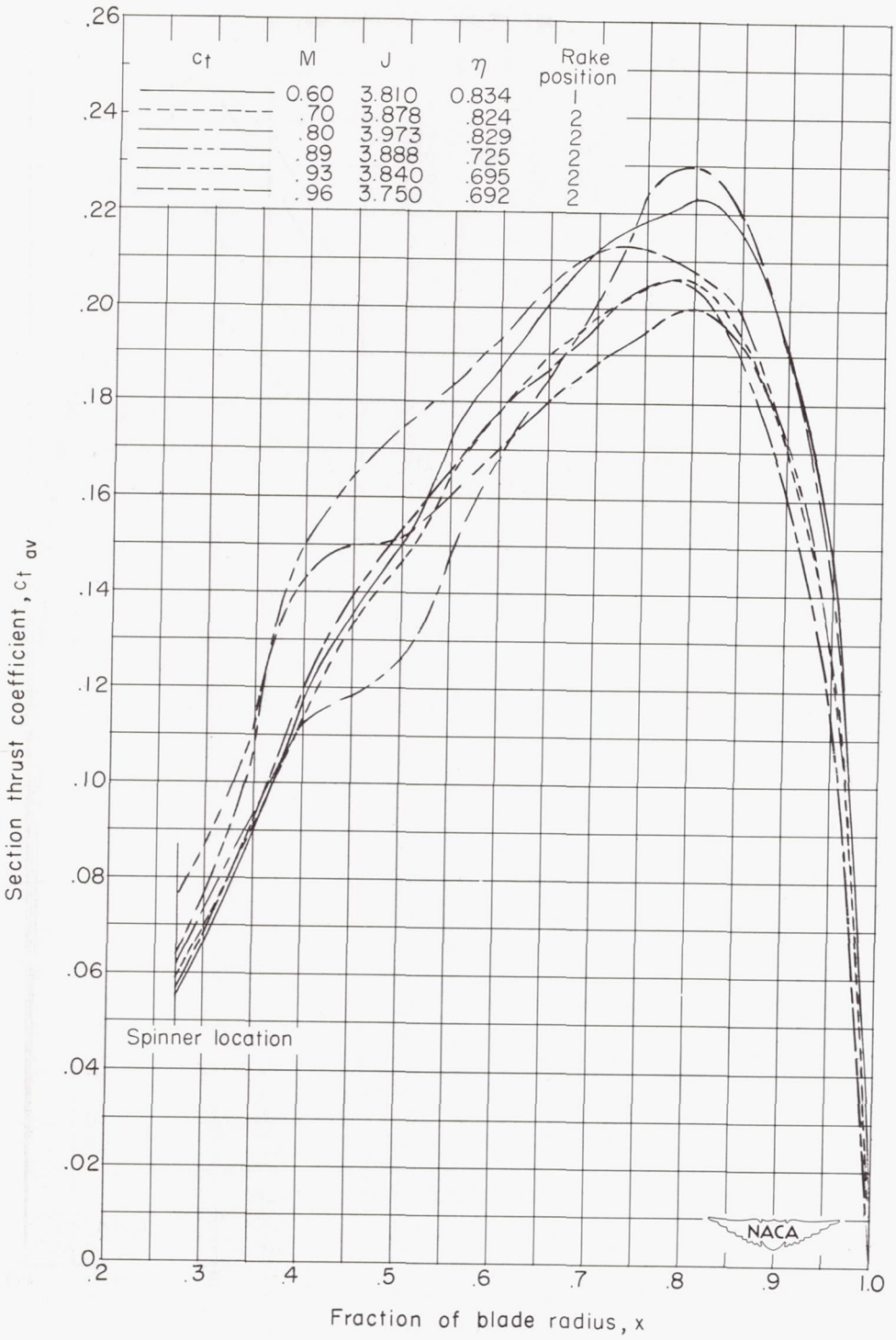

(c) $\beta_{0.75R} = 60.2^{\circ}$.

Figure 10.- Concluded.

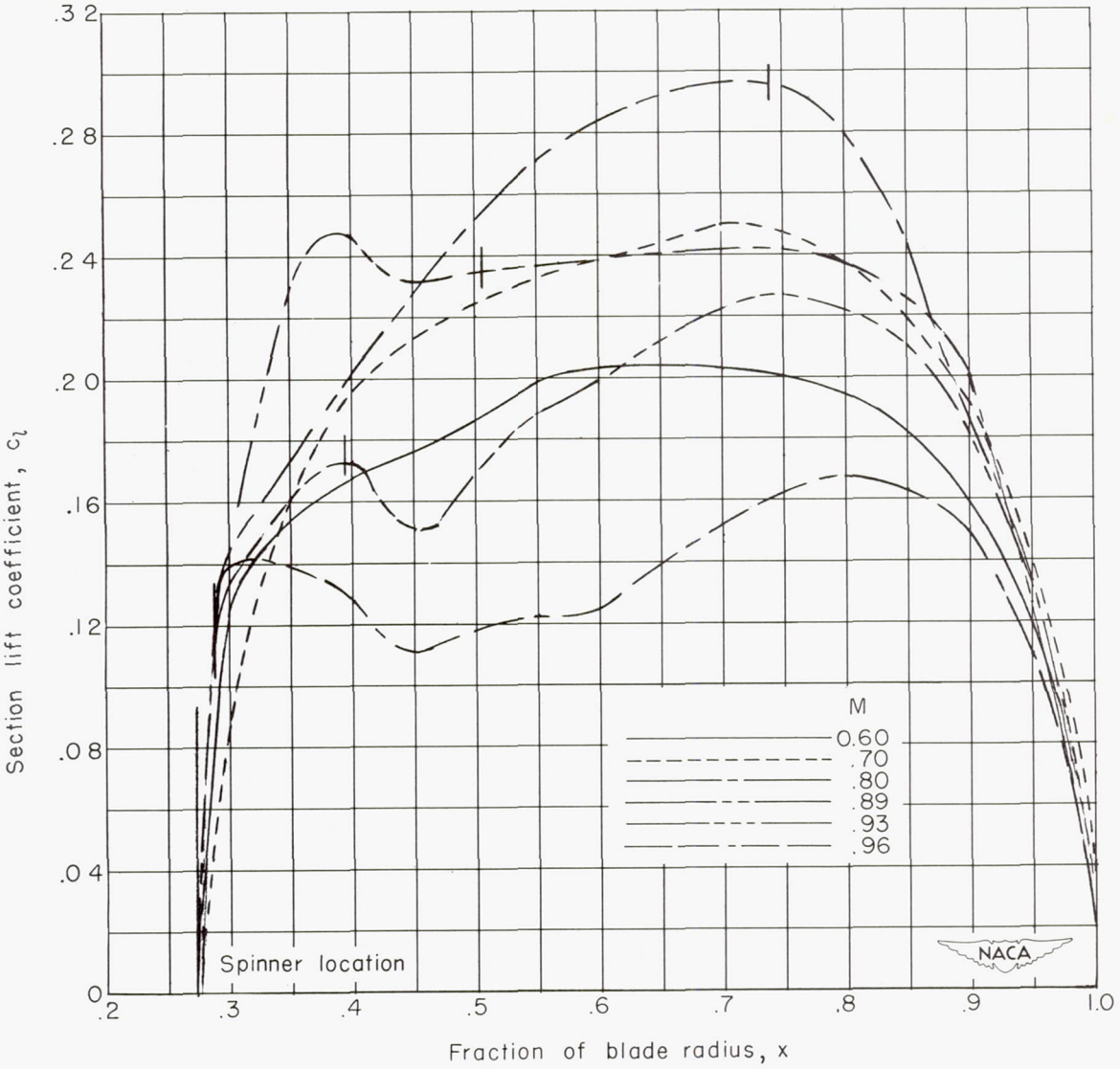

(a) Constant advance ratio of 3.10.

Figure 11.- The lift-coefficient distribution at $\beta_{0.75R} = 54.7^{\circ}$ for several Mach numbers. Ticks indicate section Mach numbers of 1.00.

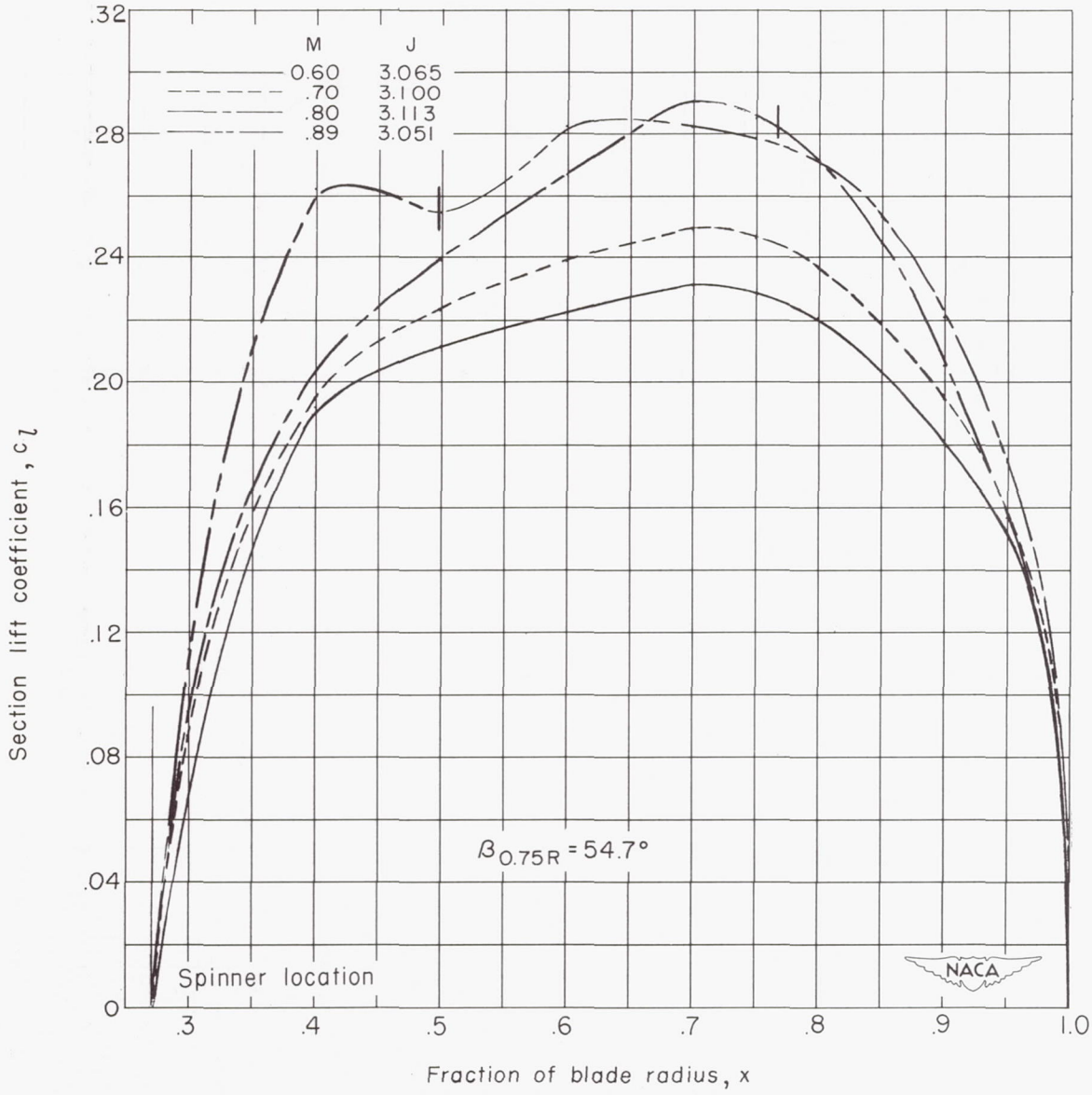

(b) Advance ratios for maximum efficiency.

Figure 11.- Concluded.

NACA-Langley - 10-30-53 - 325